Wenzhou shrimp virus 8 (WZV8) diagnosis by unique inclusions in shrimp hepatopancreatic E-cells and by RT-PCR

Jiraporn Srisala[a], Dararat Thaiue[a], Piyachat Saguanrut[a],
Suparat Taengchaiyaphum[a], Timothy W. Flegel[b,c],
Kallaya Sritunyalucksana[a],*

[a]Aquatic Animal Health Research Team, Integrative Aquaculture Biotechnology Research Group, National Center for Genetic Engineering and Biotechnology (BIOTEC), National Science and Technology Development Agency (NSTDA), Yothi Office, Rama VI Rd., Bangkok 10400, Thailand

[b]Center of Excellence for Shrimp Molecular Biology and Biotechnology (Centex Shrimp), Faculty of Science, Mahidol University, Rama VI Rd., Bangkok 10400, Thailand

[c] National Center for Genetic Engineering and Biotechnology (BIOTEC), National Science and Technology Development Agency (NSTDA), Thailand Science Park, Khlong Luang, Pathum Thani, Thailand 12120

*corresponding author: kallaya@biotec.or.th

ABSTRACT

The genome sequence of Wenzhou shrimp virus 8 (WZV8) (GenBank record KX883984.1) was described in 2015 from wide screening for RNA viruses in aquatic animals. A closely related sequence (GenBank record OK662577.1) from the whiteleg shrimp *Penaeus vannamei* was deposited in 2021 under the name *Penaeus vannamei* picornavirus (*Pv*PV). In 2021, prior to the publication of *Pv*PV, we used an RT-PCR method devised from the sequence of KX883984.1 (described herein) to screen for WZV8 in specimens of cultivated shrimp. Samples that gave positive RT-PCR results were subsequently tested by *in situ* hybridization (ISH) analysis to identify virus target tissues. Several tissues gave positive ISH results within morphologically normal nuclei. Thus, these tissues were of no use for diagnosis of WZV8 by normal histological analysis. However, unique basophilic, cytoplasmic

inclusions within vacuoles in the hepatopancreatic E-cells were also found in the same WZV8-positive shrimp specimens and can be considered pathognomonic for diagnosis of WZV8 infection using the light microscope. Although no current proof of WZV8 is the cause of disease, it is important to investigate new viruses and related tissue anomalies, even from normal cultivated shrimp, to determine whether they may have any relationship to significant negative effects on the production of cultivated shrimp.

Keywords: Wenzhou shrimp virus 8 (WZV8); *Penaeus vannamei* picornavirus (*Pv*PV); RT-PCR; histological diagnosis; pathognomonic inclusions

INTRODUCTION

Wenzhou shrimp virus 8 (WZV8) (Li et al. 2015) was discovered in 2015 by wide screening of marine animals for RNA viruses using high throughput sequencing (GenBank record KX883984.1). The full genome sequence of WZV8 is 10,455 nucleotides. A more recent publication from China (Liu et al., 2021) also gives a full genome sequence (GenBank record OK662577.1) that is highly similar to that of WZV8 (97% coverage and 95.4% sequence identity), but under the newly proposed name *Penaeus vannamei* picornavirus (*Pv*PV) with a full genome sequence of 10,550 nucleotides). Although the *Pv*PV article contained no histological analysis, it did include an electron micrograph of a cytoplasmic viral inclusion within a vacuole of an unspecified hepatopancreatic epithelial cell type (Liu et al., 2021).

After the publication reporting WZV8 (Li et al., 2015) and a subsequent publication from Australia reporting the presence of WZV8 in the transcriptome of wild *Penaeus monodon* (Huerlimann et al., 2018), we used the sequence of KX883984.1 to design an RT-PCR detection method for WZV8. We also used the same primers to prepare an *in situ* hybridization (ISH) probe for WZV8 detection in shrimp tissue sections. With shrimp samples positive for WZV8 by the RT-PCR method, we used ISH to identify unique inclusions described herein as linked to WZV8 in hematoxylin and eosin (H&E) stained tissues.

Because WZV8 is an RNA virus, archived shrimp specimens preserved in paraffin blocks for histological analysis cannot be used for ISH analysis because of the instability of RNA. Care must even be taken with a short period of fixation in Davidson's fixative to obtain reliable ISH results. Thus, in the current absence of a validated immunohistochemical method, long-storage, paraffin-embedded

tissues cannot be used for molecular analysis. These limitations do not apply to analysis of the unique lesions by H&E staining.

The purpose of this communication is to provide information allowing for the diagnosis of WZV8 infections using standard light microscope methods for examination of shrimp hepatopancreatic tissue sections stained with hematoxylin and eosin. An RT-PCR protocol to screen for WZV8 is also provided.

MATERIALS AND METHODS

Sample sources and overall research protocol

Samples from global clients from the Americas and the Indo-Pacific were used as RNA templates to develop a nested RT-PCR method for WZV8. The forward and reverse primers for the first RT-PCR and the nested PCR were designed from the sequences of GenBank record KX883984.1. This was done prior to our knowledge of the publication on *Pv*PV (Liu et al., 2021) and submission of its genome sequence (OK662577.1) to GenBank. The amplicons amplified from three specimens from the Indo-Pacific (SG1.1, SG1.2, and SG 1.3) and from the Americas (SG2.1, SG2.2, and SG2.3) were subjected to sequencing and bioinformatics analysis.

Histological analysis

Standard methods were used for shrimp fixation and processing to prepare hematoxylin and eosin (H&E) stained tissue sections (Bell and Lightner, 1988). These were analyzed using a Leica ICC50 HD digital light microscope. For semi-thin sections, tissue samples were removed from the outer, E-cell region of the hepatopancreas for fixation in 4% glutaraldehyde solution (4% glutaraldehyde, 19 mM $NaH_2PO_4 \cdot H_2O$, 81 mM Na_2HPO_4, pH 7.4), embedded in epoxy resin, sectioned using a Leica EM UC6 ultramicrotome with a glass knife and stained with toluidine blue as previously described (Sriurairatana et al., 2014).

RT-PCR method

The first step RT-PCR reaction is performed in 12.5 µl mixture consisting of 1X Reaction Mix (Invitrogen, USA), 0.4 µM each of WZV8-482F and WZV8-482R primers (**Table 1**), 0.5 µl of SuperScript III RT/Platinum Taq Mix (Invitrogen, USA) and 100 ng of RNA template. The RT-PCR protocol begins with 50°C for 30 min followed by 94°C for 2 min and then by 35 cycles of 94°C for 30 sec, 60°C for 30 sec and 68°C for 45 sec plus a final extension at 68°C for 5 min. For the nested PCR step, the 12.5 µl mixture contains 1X OneTaq Hot Start Master Mix (NEB, USA), 0.2 µM of each

98 WZV8-168F and WZV8-168R primer (Table 1), and l µl of the product solution from the first RT-
99 PCR step. The nested PCR protocol is 94°C for 5 min, followed by 25 cycles of 94ºC for 30 sec, 60ºC
100 for 30 sec and 72ºC for 30 sec plus a final extension for 5 min at 72 ºC. The amplicons yielded are 482
101 bp and 168 bp, respectively.
102
103 **Table 1**. Primers used for the nested RT-PCR detection method for WZV8 developed in this study.
104

Method	Primer name	Sequence (5'-3')	Amplicon size (bp)
First RT-PCR	WZV8-482F	ATGCCTCTGGAAAGCGATAC	482
	WZV8-482R	GGTGTTAGATCGCTCCTTCTTC	
Nested PCR	WZV8-168F	GAAAGCGATACTCCTACGACAG	168
	WZV8-168R	TCTTGAGTTTGAGGAAGGTGAG	

105
106 ***Bioinformatics analysis***
107 Multiple sequences alignment of amplicons SG1.1, SG1.2, SG1.3, SG2.1, SG2.2, and SG2.3 was
108 performed by Clustal Omega (https://www.ebi.ac.uk/Tools/msa/clustal/) and nucleotide sequence
109 similarity was analyzed using the BLASTn sequence analysis tool
110 (https://blast.ncbi.nlm.nih.gov/Blast.cgi). The phylogenetic tree was constructed using MEGA 7
111 program. Tree topology was evaluated using bootstrap analysis by the neighbor joining method with
112 default parameters for 1000 replicates.
113
114 ***In situ* hybridization (ISH)**
115 ISH assays were carried out as previously described (Srisala et al., 2021). The primers WZV8-482F
116 and WZV8-482R (Table 1) were used with a plasmid template containing a WZV8 genome fragment
117 to prepare a DIG-labeled WZV8 probe. Our negative control specimens consisted of shrimp that were
118 negative for WZV8 by RT-PCR and also showed no WZV8 inclusions. Each ISH included 3 adjacent
119 tissue sections, one for H&E staining, one for the ISH probe and one for a no-probe control.
120
121 **RESULTS AND DISCUSSION**
122 **Nested RT-PCR detection of WZV8**
123 The primers designed for WZV8 were based on the nucleotide sequence record of GenBank accession
124 no. KX883984.1. A schematic diagram representing primer regions specific to a portion upstream (nt
125 3889-nt 4370) of the putative RNA-dependent RNA polymerase (RdRp) is shown in **Fig. 1**. The

sensitivity of the method is 20 copies per reaction vial using purified WZV8 amplicons as the template. An agarose gel showing RT-PCR amplicons obtained from 3 samples each from the Indo-Pacific (SG1.1, SG1.2, and SG 1.3) and the Americas (SG2.1, SG2.2, and SG2.3) is shown in **Fig. 2**.

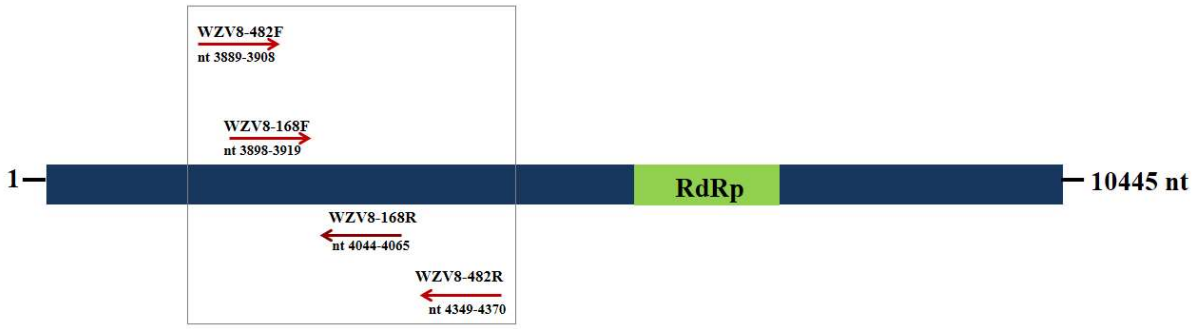

Figure 1. A schematic diagram representing primer regions upstream of RdRP gene. The red arrows indicate the locations of the primers for the first RT-PCR step: WZV8-482F and WZV8-482R, and the nested PCR step: WZV8-168F and WZV8-168R. The nucleotide positions of the primers according to the position of the GenBank record KX883984.1 are shown.

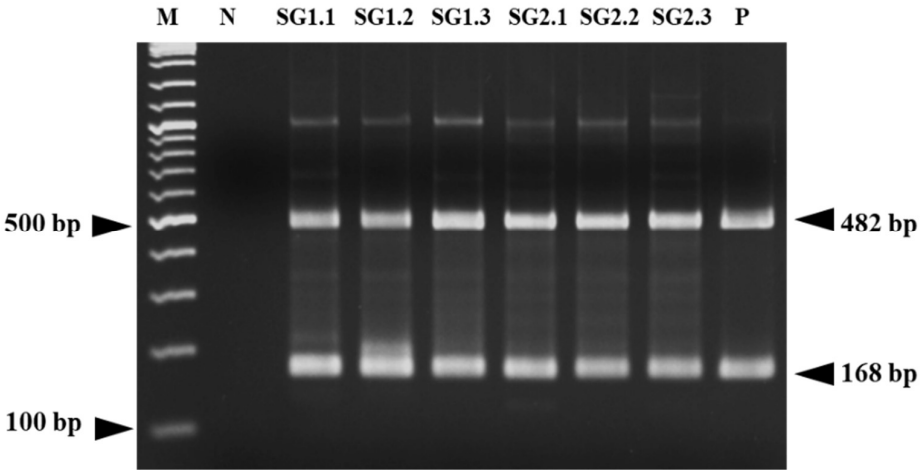

Figure 2. Photograph of an agarose gel showing RT-PCR amplicons obtained from 6 shrimp specimens using the WZV8 method. M = 2 log DNA marker; N = Negative control; P = Positive control.

A Clustal Omega alignment of the consensus sequences of these amplicons with WZV8 sequence (GenBank record KX883984.1) and the *Pv*PV sequence (GenBank record OK662577.1) is shown in **Supplementary Fig. S1.** The % identity among the eight nucleotide sequences differed appreciably (**Table 2**), even for the two GenBank sequences from China (93.3-98.1%). This indicates relatively

high variability in only 6 different WZV8 samples that may possibly differ in virulence for shrimp. Phylogenetic analysis revealed that the WZV8 sequences of the Indo-Pacific specimens (SG1) fell in a clade with the Chinese sequences and separated from the American sequences (SG2) **(Fig. 3**).

Table 2. Percent identity matrix among the eight aligned nucleotide sequences created by Clustal Omega program.

	SG1.1	SG1.2	SG1.3	SG2.1	SG2.2	SG2.3	OK662577.1	KX883984.1
SG1.1	100.0							
SG1.2	92.9	100.0						
SG1.3	93.1	99.7	100.0					
SG2.1	93.9	92.9	93.1	100.0				
SG2.2	93.7	93.5	93.7	99.3	100.0			
SG2.3	92.9	91.7	91.9	97.7	97.5	100.0		
OK662577.1	95.6	94.4	94.6	93.9	94.6	93.3	100.0	
KX883984.1	96.6	95.6	95.8	94.8	95.4	94.1	98.1	100.0

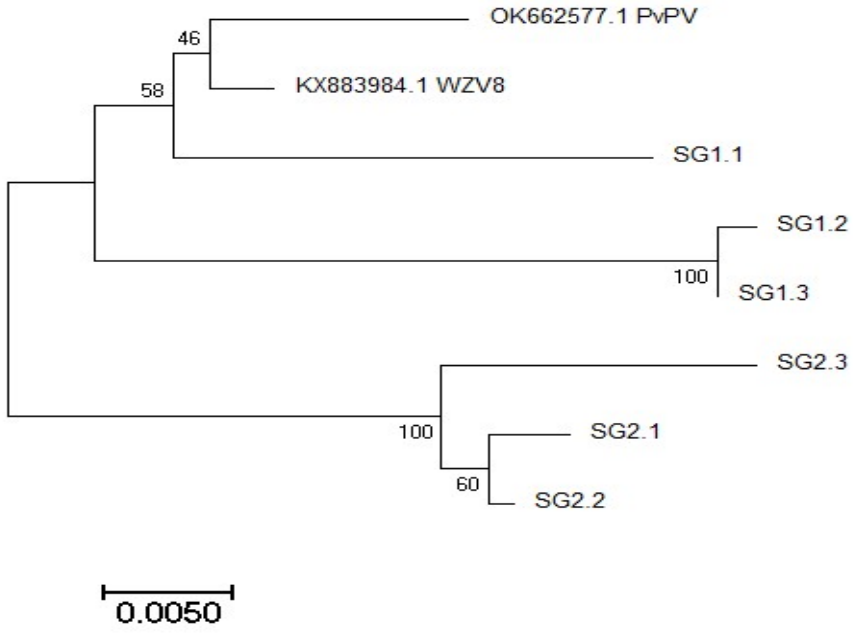

Figure 3. Phylogenetic tree based on RT-PCR amplicon sequences of 6 shrimp specimens compared to matching regions of WZV8 and *Pv*PV nucleotide sequences at GenBank. The tree was constructed using the neighbor-joining method with MEGA 7 software. The percentages of replicate trees in which the associated taxa clustered together in the bootstrap test (1000 replicates) are shown next to the branches.

185 Since our RT-PCR method was developed based on the GenBank record KX883984.1, it may not be
186 suitable for detection of all types of WZV8 that exist, but we found it useful for specimens from Asia
187 to the Americas and it may serve as a preliminary method until a more universal method can be
188 developed, perhaps to cover all variants. Upon request to the corresponding author, we are willing to
189 provide a free plasmid containing the target for our method. It can be used to transform *E. coli* as a
190 perpetual source of a positive control plasmid for PCR tests and for use as a template to prepare ISH
191 probes. With proper acknowledgement of the source, the plasmid may be distributed freely without
192 seeking prior permission. We wish this tool to be distributed as widely and quickly as possible to
193 encourage cooperation and exchange of information on WZV8-like viruses.
194
195 **Identification of WZV8 inclusions by *in situ* hybridization**
196 Our first set of shrimp positive for WZV8 by RT-PCR were processed for histological analysis by
197 H&E staining and by ISH analysis using a DIG-labeled probe prepared by PCR using the plasmid
198 containing the WZV8 target sequence. Prior to our ISH tests, we did not know the target tissue for
199 WZV8 except for one electron micrograph in the paper on *Pv*PV (Liu et al. 2021) showing a viral
200 inclusion in a vacuole of an unidentified HP cell. Examples of positive ISH reactions for WZV8 in an
201 HP sample are shown (black arrows) in a low magnification photomicrograph (**Fig. 4**). These positive
202 ISH reactions are predominantly in E-cells that are located at the distal ends of HP tubules rather than
203 in the medial region (asterisks). A portion of this photomicrograph (box outline) is shown at higher
204 magnification in **Fig. 5**, where 2 of the positive ISH signals in E-cells arise from circular inclusions
205 within vacuoles, i.e., morphology like the basophilic inclusions subsequently seen in E-cells with H&E
206 staining. Also in Fig. 5 is an E-cell with a positive ISH reaction in both the nucleus and cytoplasm of
207 a cell that has otherwise normal morphology and was not be recognizable as an infected cell by H&E
208 staining. Additional ISH positive circular inclusions within vacuoles in the cytoplasm of E-cells are
209 shown in **Fig. 6** collected from other samples. Further work using transmission electron microscopy
210 (TEM) will be necessary to determine the reasons for differences in morphology for ISH-positive cells.
211 Our shrimp samples that tested negative for WZV8 by RT-PCR did not show such inclusions or any
212 ISH positive results (not shown). In the next section, semi-thin sections stained with toluidine blue are
213 also included for comparison to the H&E-stained tissues.
214
215
216
217

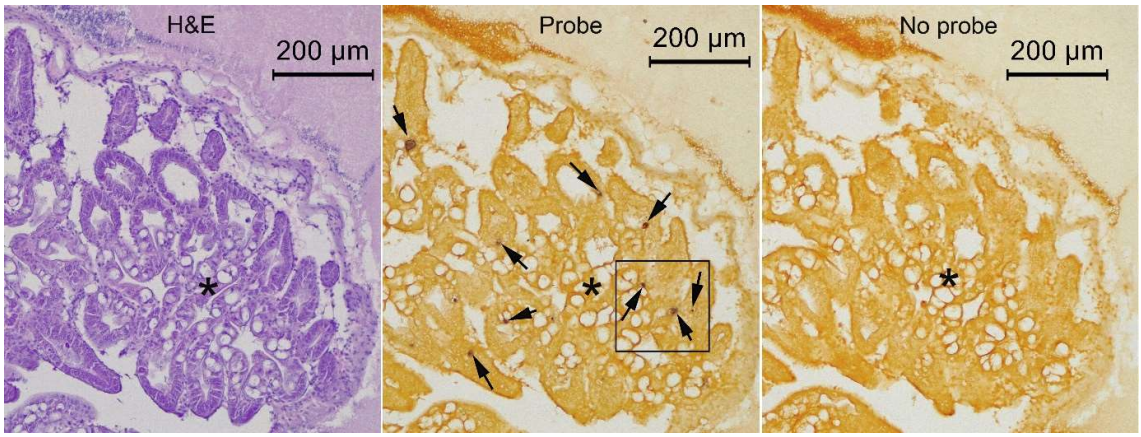

Figure 4. Low magnification photomicrographs from an ISH assay, showing positive ISH reactions (black arrows). These are often found predominantly in E-cells and less frequently in areas (asterisks) of differentiated HP tubule epithelial cells characterized by the presence of vacuoles. The box in the middle of photomicrograph is shown at higher magnification in Fig. 5.

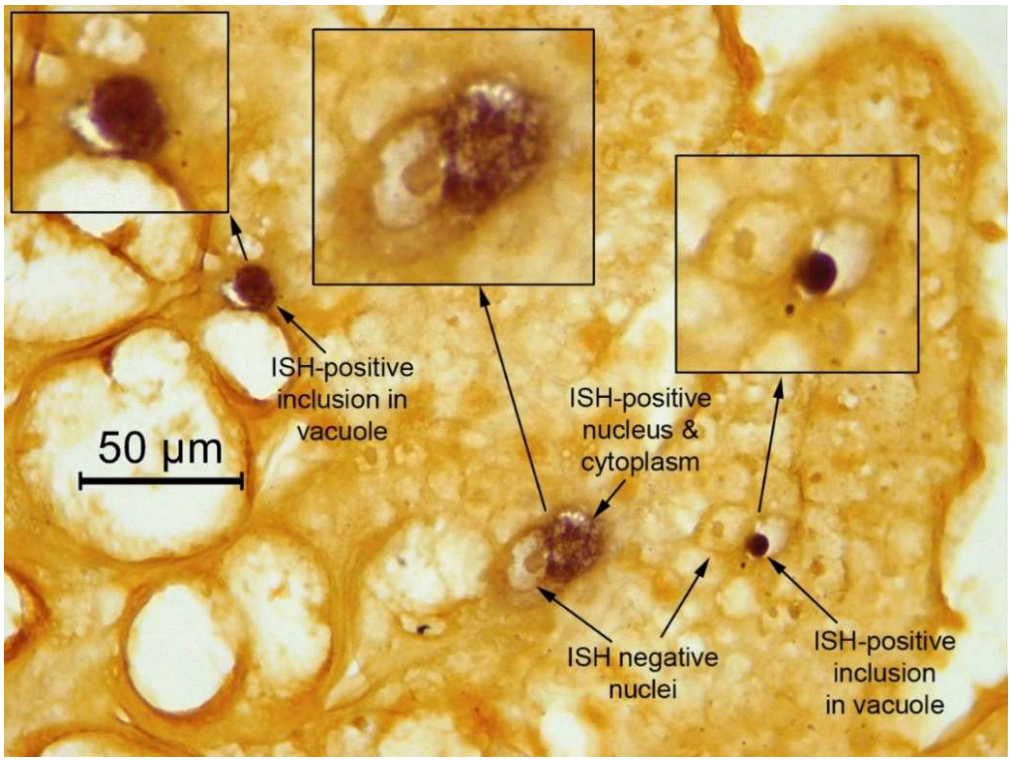

Figure 5. Magnification of the box in Fig. 4 showing 2 positive ISH reactions as dark, circular positive signals in vacuoles, resembling the position and shape of basophilic inclusions seen in vacuoles with H&E staining. Also shown is another ISH positive cell with no circular inclusion but instead positive ISH reactions in both the nucleus and cytoplasm. This positive cell did not differ from other normal cells with H&E staining.

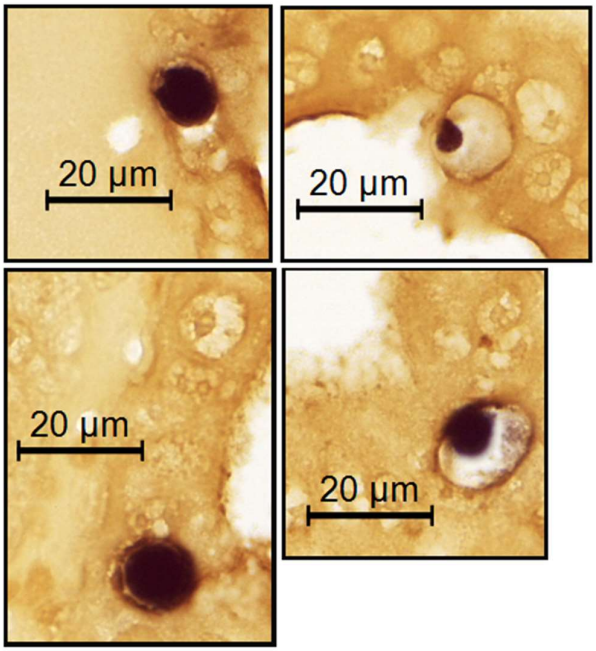

Figure 6. A collection of 4 photomicrographs from various samples showing high magnifications of ISH positive reactions with circular inclusions within vacuoles of E-cells. The sizes of the inclusions range from approximately 3 to 11 µM.

In some specimens positive for WZV8 by PCR, there were occasionally ISH positive nuclei of normal morphology within normal tubule epithelial cells in the medial and proximal areas of the HP and in the subcuticular epithelium, especially in the stomach (**Supplementary Fig. S2-S4**). The matching H&E-stained tissues had normal morphology. These reactions were sometimes present without or together with E-cells showing ISH reactions in circular inclusions within vacuoles of E-cells. We are uncertain about the nature of these ISH reactions but hope that TEM may provide some insight. In addition, it is possible that they might arise from endogenous viral elements (EVE) of WZV8 within the genomic DNA of the respective RT-PCR positive specimens.

Characteristics of WZV8 inclusions in H&E-stained tissues

After seeing the positive ISH reactions predominantly in the cytoplasm of E-cells, we examined the adjacent tissue sections stained with hematoxylin and eosin (H&E) for abnormal, circular, cytoplasmic inclusions in vacuoles of these cells. Thus, we discovered cytoplasmic, deeply basophilic inclusions that were circular in section and were often contained within a cytoplasmic vacuole (**Figs. 7 and 8**). They should not be confused with metaphase plates in plane section (**Fig. 9**) commonly seen in E-cells where there is a high rate of cell division. Although the deeply basophilic, circular inclusions of WZV8

were dominant, there were also variations in their appearance. For example, they were sometimes associated with a nearby or attached, eosinophilic, circular inclusion, usually of smaller size (**Fig. 10**) (i.e., "double-inclusions"). Sometimes the circular basophilic inclusions were seen in differentiated HP tubule epithelial cells, and an example photomicrograph of WZV8 inclusions in R-cells is shown in **Fig. 11**. In addition, the double-inclusions were sometimes separated by an unstained space from a surrounding basophilic to magenta colored "surround" of variable thickness that was itself surrounded by an unstained space. We are uncertain as to the steps in development of the "surround" but speculate that it may consist of the whole cell cytoplasm that has shrunken away from adjacent cells. Hopefully, TEM will clarify this issue.

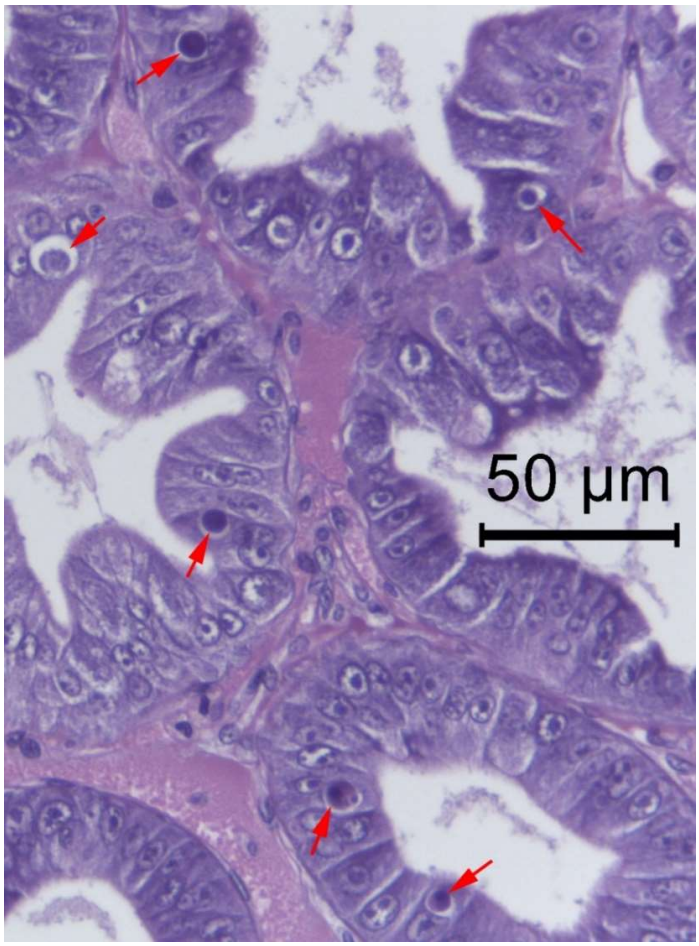

Figure 7. Photomicrograph taken using a 40x objective showing E-cells of the shrimp hepatopancreas containing WZV8 cytoplasmic inclusions within vacuoles (red arrows). They have variable morphology and staining properties. The dominant ones are deeply basophilic and mostly perfectly circular. The lightly basophilic inclusion on the upper far left may be an early developmental stage, while the bottom two are more complex and show some eosinophilic staining in addition to a central, circular, densely basophilic inclusion.

Figure 8. Example photomicrographs of the most common, circular, lightly to deeply basophilic, cytoplasmic inclusions of WZV8 within vacuoles in E-cells.

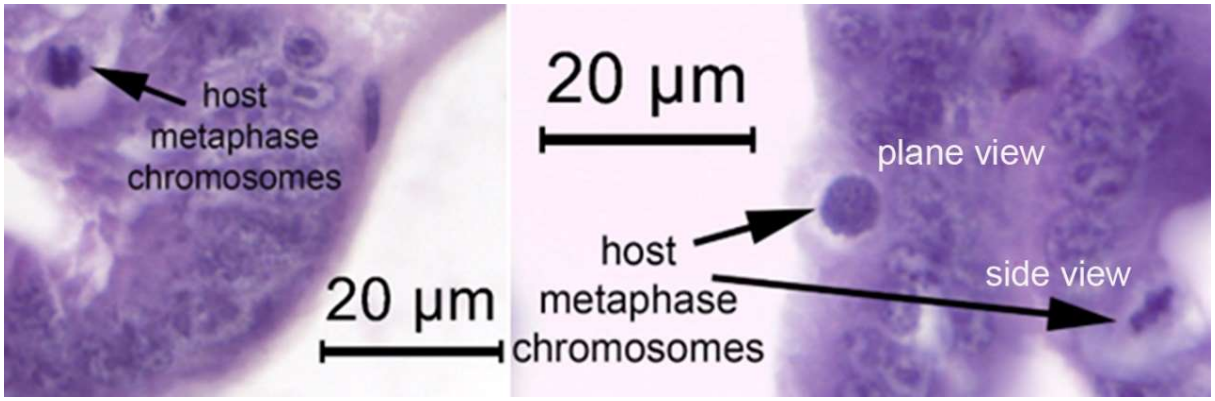

Figure 9. Example photomicrographs of metaphase chromosomes in E-cells that may sometimes resemble WZV8 inclusions when the tissue section passes through the plane of the metaphase plate rather than the side. One must be careful not to confuse these with WZV8 inclusions.

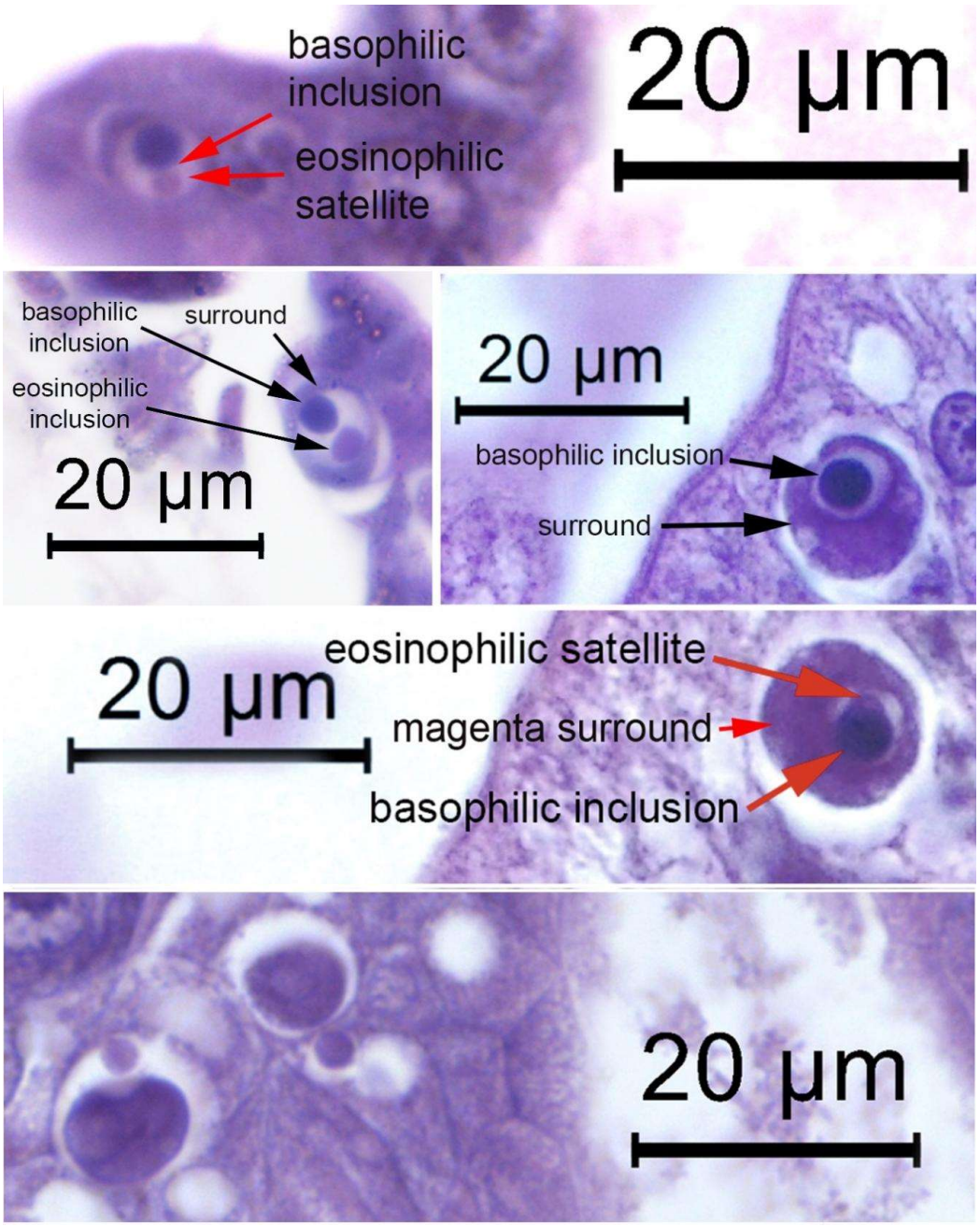

Figure 10. Variations in basophilic WZV8 inclusions that are sometimes accompanied by usually smaller, circular, eosinophilic satellite inclusions. This is a highly distinctive combination, such that "densely basophilic, circular inclusions accompanied by a closely associated satellite, eosinophilic inclusion within an E-cell vacuole" may be considered pathognomonic for WZV8.

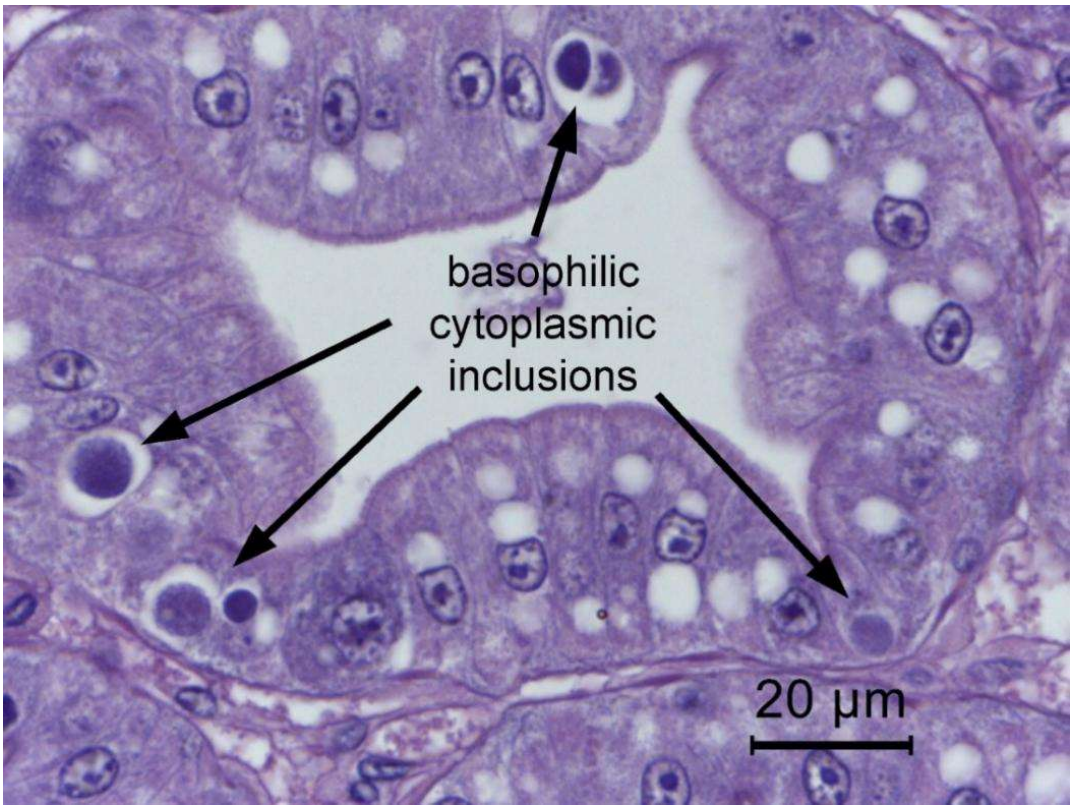

Figure 11. Photomicrograph of WZV8 basophilic inclusions in differentiated cells (R-cells) of the shrimp hepatopancreas.

The double-inclusions consisting of a basophilic and eosinophilic partner may be common, but the eosinophilic partners are mostly small in comparison to the larger basophilic inclusion such that the probability of them appearing together in 4-micron tissue sections would be small. Thus, it is difficult to determine whether this unique pairing occurs regularly or is of low occurrence. More work is needed to determine the relationship among these variable inclusions and how they develop. Hopefully, transmission electron microscopy (TEM) will help to achieve this goal.

Photomicrographs of semi-thin sections of WZV8 inclusions in E-cells are also shown in **Fig. 12** stained with toluidine blue. The double-inclusions are so distinctive in their nature by both H&E staining and in semi-thin sections that their occurrence, together with their common location in E-cells may be considered pathognomonic for WZV8 infection. We propose calling these unique inclusions "Lightner double inclusions" (LDI) to honor recently deceased Prof. Donald V. Lightner to whom we are greatly indebted for his monumental contributions in the field of shrimp pathology.

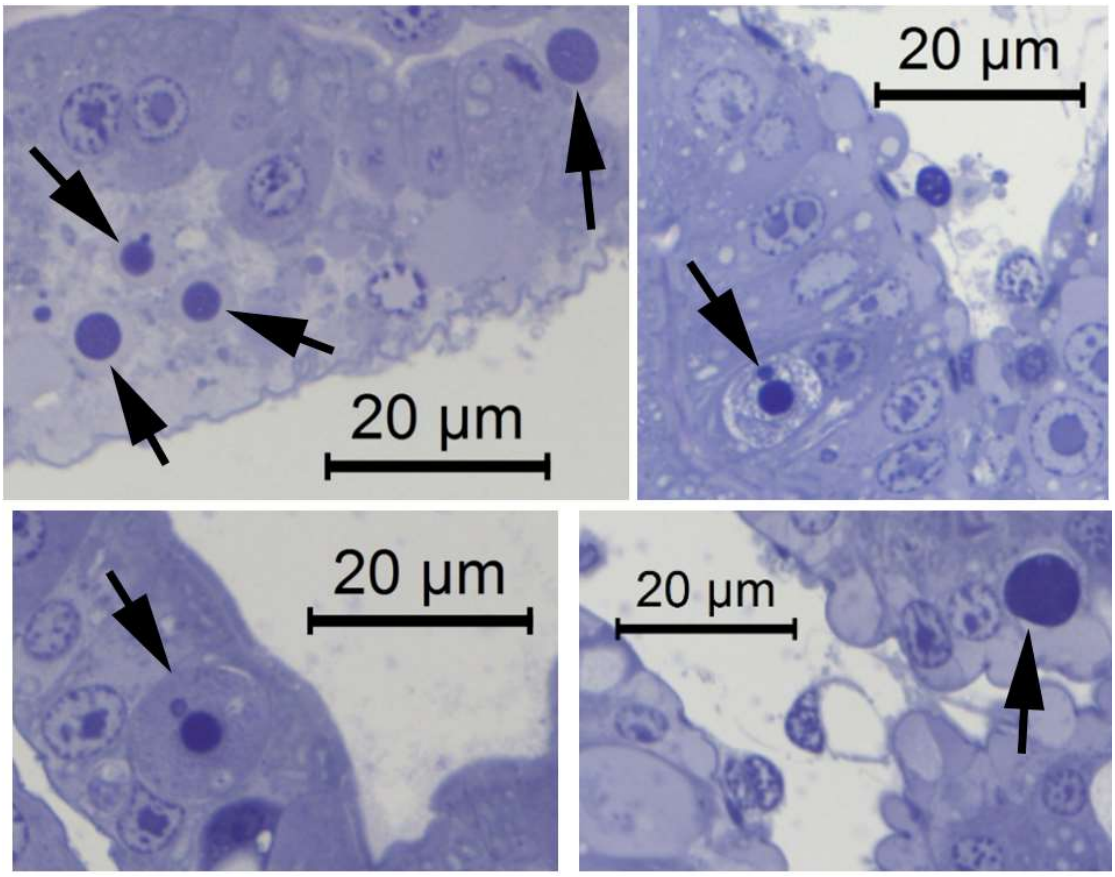

Figure 12. Photomicrographs of semi-thin sections of shrimp HP tissue showing variation in WZV8 inclusions (dark blue and circular) in E-cells of the shrimp hepatopancreas. Some show a smaller, adjacent satellite inclusion or other vacuolar contents.

Retrospective on WZV8 inclusions

In retrospect, we had previously seen WZV8 inclusions in both *Penaeus monodon* and *P. vannamei* from several shrimp farming countries in Austral-Asia since at least 2008. They were described in histological reports to clients as of unknown origin. More recently we obtained samples of *P. vannamei* from the Americas that also showed these inclusions. We regarded them as "mystery inclusions" that we originally speculated might be developmental stages of the microsporidian *Enterocytozoon hepatopenaei* (EHP). However, the "mystery inclusions" were subsequently found to be negative for EHP using a specific *in situ* hybridization (ISH) probe for EHP. In addition, we had already discovered by histological analysis and ISH assays that EHP does not infect E-cells (Flegel, 2012; Chaijarasphong et al., 2020). Thus, the inclusions remained a mystery.

In most cases, occurrence of the "mystery inclusions" was not associated with disease. When they were present in diseased shrimp, they occurred together with other, known lethal pathogens (bacteria

470 or viruses) that were deemed the cause of morbidity. Lacking a clear link to disease and being sporadic
471 in occurrence, we regarded them somewhat as a curiosity that was not pursued due to other more urgent
472 work.
473
474 The original publication describing WZV8 did not include information related to signs of disease,
475 histopathology or pathogenicity (Li et al. 2015). Nor did the publication on PvPV (Liu et al. 2021).
476 However, to confirm virulence, isolation of a new virus from moribund shrimp must be accompanied
477 by histopathological analysis for the presence of other known pathogens together with results from
478 challenge tests employing the new purified virus to show that it alone can produce the same
479 histopathology as seen in the original diseased shrimp. To date, there is no proof that WZV8-related
480 viruses have caused disease, and we have many histological samples from normal shrimp dating back
481 over a decade that show the distinctive WZV8 Lightner double inclusions (LDI). This suggests that
482 WZV8-like viurses may have had little impact on production of cultivated *P. monodon* and *P.*
483 *vannamei*.
484
485 Despite historical evidence indicating lack of virulence, it is possible that many types of WZV8 exist
486 and that some may be lethal or may contribute to mortality in combination with one or more other
487 pathogens or under some environmental conditions. This is what needs to be established as quickly as
488 possible. Thus, it is important to mobilize researchers in all shrimp rearing countries to assess the
489 distribution and potential virulence of WZV8-like viurses. We hope that retrospective review of
490 existing histological samples for LDI together with RT-PCR screening of fresh material will lead to
491 rapid acquisition of new information and to the development of a more universal RT-PCR detection
492 method. At the same time, it is important to keep in mind that a rapid rise in reports of WZV8
493 occurrence will not be an indication of viral spread but simply the discovery of its current range. This
494 virus has been around for at least a decade or more with no apparent link to disease.
495
496 **Acknowledgement:** This research project is supported by Mahidol University (Fundamental Fund:
497 Basic Research Fund: fiscal year 2022) (Grant no. BRF1-054/2565) and the NSRF via the Program
498 Management Unit for Human Resources & Institutional Development, Research and Innovation
499 (B05F640137). We also thank Agricultural Research Development Agency (ARDA), Thailand
500 (PRP6505030760) to Kallaya Sritunyalucksana.
501
502 **REFERENCES**

503 Bell, T.A., Lightner, D.V., 1988. A handbook of normal shrimp histology. World Aquaculture
504 Society, Baton Rouge, LA.
505 Chaijarasphong, T., Munkongwongsiri, N., Stentiford, G.D., Aldama-Cano, D.J., Thansa, K., Flegel,
506 T.W., Sritunyalucksana, K., Itsathitphaisarn, O., 2020. The shrimp microsporidian
507 *Enterocytozoon hepatopenaei* (EHP): Biology, pathology, diagnostics and control. J. Invertebr.
508 Pathol., 107458.
509 Flegel, T.W., 2012. Historic emergence, impact and current status of shrimp pathogens in Asia. J.
510 Invertebr. Pathol. 110, 166-173.
511 Huerlimann, R., Wade, N.M., Gordon, L., Montenegro, J.D., Goodall, J., McWilliam, S., Tinning,
512 M., Siemering, K., Giardina, E., Donovan, D., 2018. De novo assembly, characterization,
513 functional annotation and expression patterns of the black tiger shrimp (*Penaeus monodon*)
514 transcriptome. Sci. Rep. 8, 1-14.
515 Li, C.-X., Shi, M., Tian, J.-H., Lin, X.-D., Kang, Y.-J., Chen, L.-J., Qin, X.-C., Xu, J., Holmes, E.C.,
516 Zhang, Y.-Z., 2015. Unprecedented genomic diversity of RNA viruses in arthropods reveals the
517 ancestry of negative-sense RNA viruses. eLife. 4, e05378.
518 Liu, S., Xu, T., Wang, C., Jia, T., Zhang, Q., 2021. A novel picornavirus discovered in white leg
519 shrimp *Penaeus vannamei*. Viruses. 13, 2381.
520 Sriurairatana, S., Boonyawiwat, V., Gangnonngiw, W., Laosutthipong, C., Hiranchan, J., Flegel,
521 T.W., 2014. White feces syndrome of shrimp arises from transformation, sloughing and
522 aggregation of hepatopancreatic microvilli into vermiform bodies superficially resembling
523 gregarines. PLoS One. 9, e99170.
524
525
526
527
528
529
530
531
532
533
534
535
536

SUPPLEMENTARY INFORMATION

```
SG1.1          ATGTCTCTGGAAAGCGATACACCTACGACAGCGAAAAGTTCATCACTCGCGTGACCACCA    60
SG1.2          ATGCCTCTGGAAAGCGATACTCCTACGATAGCGATACATTCATCACTCGCGTGACCACCA    60
SG1.3          ATGCCTCTGGAAAGCGATACTCCTACGATAGCGATACATTCATCACTCGCGTGACCACCA    60
SG2.1          ATGCCTCTGGAAAGCGATACACTTACGACAGTGAGACCTTCATCACCCGCGTGACTACCA    60
SG2.2          ATGCCTCTGGAAAGCGATACACCTACGACAGTGAGACCTTCATCACCCGCGTGACTACCA    60
SG2.3          ATGCCTCTGGAAAGCGATACACCTACGACAGTGAGACCTTCATCACCCGCGTGACTACCA    60
OK662577.1     ATGCCTCTGGAAAGCGATATACCTATGACAGTGAGAAGTTCATCACTCGCGTGACCACCA    60
KX883984.1     ATGCCTCTGGAAAGCGATACTCCTACGACAGCGAGAAGTTCATCACTCGCGTGACCACCA    60
               *** ****************  * ** ** ** ** *  ******** ******** ****

SG1.1          CCCTTCAAGACGTCAGCTACTGGCAGGGTCTCCCGCTAGAAGCCATCATCTACCTCATGA   120
SG1.2          CTCTTCAAGACGTCAGCTACTGGCAGGGTCTCCCACTAGAAGCCATCATCTACCTCATGA   120
SG1.3          CTCTTCAAGACGTCAGCTACTGGCAGGGTCTCCCACTAGAAGCCATCATCTACCTCATGA   120
SG2.1          CCCTTCAAGACGTCAGCTACTGGCAGGGTCTCCCGCTAGAAGCCATCATCTACCTCATGA   120
SG2.2          CCCTTCAAGACGTCAGCTACTGGCAGGGTCTCCCGCTAGAAGCCATCATCTACCTCATGA   120
SG2.3          CCCTTCAAGACGTCAGCTACTGGCAGGGCCTCCCGCTAGAAGCTATCATCTACCTCATGA   120
OK662577.1     CCCTTCAAGACGTCAGCTACTGGCAGGGCCTCCCGCTAGAAGCCATCATCTACCTCATGA   120
KX883984.1     CCCTTCAAGACGTCAGCTACTGGCAGGGCCTCCCGCTAGAAGCCATCATCTACCTCATGA   120
               * ************************** ***** ******** ****************

SG1.1          AGAATCACCAAGTCATCATCGAAGAGCACTTTCCCCTCACCTTCCTCAAGCTCAAGAAGA   180
SG1.2          AGAATCATCAAGTCATCATCGAAGAGCACTTCCCCCTCACCTTCCTCAAACTCAAGAAGA   180
SG1.3          AGAATCATCAAGTCATCATCGAAGAGCACTTCCCCCTCACCTTCCTCAAACTCAAGAAGA   180
SG2.1          AGAATCACCAAGTCATCATCGAAGAGCACTTCCCCCTCACCTTCCTCAAACTCAAGAAGA   180
SG2.2          AGAATCACCAAGTCATCATCGAAGAGCACTTCCCCCTCACCTTCCTCAAACTCAAGAAGA   180
SG2.3          AGAATCACCAAGTCATCATCGAAGAGCATTTCCCCCTCACCTTCCTCAAACTCAAGAAGA   180
OK662577.1     AGAATCATCAAGTCATCATCGAAGAGCACTTTCCCCTCACCTTCCTCAAACTCAAGAAGA   180
KX883984.1     AGAATCATCAAGTCATCATCGAAGAGCACTTCCCCCTCACCTTCCTCAAACTCAAGAAGA   180
               ******* ******************** ** ***************** **********

SG1.1          AGGCCCGCCGAGATAGAAATATGCAGATCGTCCAACAGATCACTAACTCCAAGGCCTTCC   240
SG1.2          AGGCCCGCCGAGATAGAAACCTGCAGATCGTCCAACAGATCACTAACTCTAAGGCCTTCA   240
SG1.3          AGGCCCGCCGAGATAGAAACCTGCAGATCGTCCAACAGATCACTAACTCTAAGGCCTTCA   240
SG2.1          AGGCCCGTCGAGACAGAAACATGCAGATCGTCCAACAGATCACTAACTCCGACGCCTTCA   240
SG2.2          AGGCCCGTCGAGACAGAAACATGCAGATCGTCCAACAGATCACTAACTCCGACGCCTTCA   240
SG2.3          AGGCCCGTCGAGACAGAAACATGCAGATCGTCCAACAGATCACTAACTCCGACGCCTTCA   240
OK662577.1     AGGCCCGCAGAGATAGAAACATGCAGATCGTCCAACAGATCACTAACTCCAAGGCCTTCC   240
KX883984.1     AGGCCCGCCGAGATAGAAACATGCAGATCGTCCAACAGATCACTAACTCCAAGGCCTTCC   240
               *******  **** *****  ****************************  * ******

SG1.1          AGGTTGGGTTCCCCATCGCTGTGATCGGAGTTGCTGCTACAGCAATCTTCGGGATCGCGA   300
SG1.2          AGGTTGGGTTCCCCATCGCTGTGATCGGAGTTGCTGCTACTGCAATCTTCGGAATCGCGA   300
SG1.3          AGGTTGGGTTCCCCATCGCTGTGATCGGAGTTGCTGCTACTGCAATCTTCGGGATCGCGA   300
SG2.1          AGATTGGGTTCCCCATCGCTGTGATTGGAGTTGCTGCTACAGCAATCTTCGGGATCGCGA   300
SG2.2          AGATTGGGTTCCCCATCGCTGTGATTGGAGTTGCTGCTACAGCAATCTTCGGGATCGCGA   300
SG2.3          AGATTGGGTTCCCCATCGCTGTGATTGGAGTTGCTGCCACAGCAATCTTCGGGATCGCGA   300
OK662577.1     AGGTTGGGTTCCCCATCGCTGTGATCGGAGTTGCCGCTACAGCAATCTTCGGGATCGCGA   300
KX883984.1     AGGTTGGGTTCCCCATCGCTGTGATCGGAGTTGCTGCTACAGCAATCTTCGGGATCGCGA   300
               ** ********************** ******** ** ** *********** *******

SG1.1          AACTTTCCTCCAAGAAAGAAAAGTCCCCTAAGAAACCCTCCCGACCTGACAGCGACAGCT   360
SG1.2          AACTCTCCTCCAAGAAAGAAAAGTCCCCAAAGAAGTCCTCCCAGCCTGACAGCGACAGCT   360
SG1.3          AACTCTCCTCCAAGAAAGAAAAGTCCCCAAAGAAGTCCTCCCAGCCTGACAGCGACAGCT   360
SG2.1          AACTCTCCTCCAAGAAAGAAAAGCCCCCAAAGAAACCCTCCCACCATGACAGCGACAGCT   360
SG2.2          AACTCTCCTCCAAGAAAGAAAAGCCCCCAAAGAAACCCTCCCACCATGACAGCGACAGCT   360
SG2.3          AACTCTCCTCCAAGAAAGAAAAGCCCCCAAAGAAACCCTCCCACCATGACAGCGACAGCT   360
OK662577.1     AACTCTCCTCCAAGAAAGAAAAGTCCCCAAAGAAACCCTCCCCACCTGACAGCGACAGCT   360
KX883984.1     AACTCTCCTCCAAGAAAGAAAAGTCCCCAAAGAAACCCTCCCGACCTGACAGCGACAGCT   360
               **** ******************* **** *****  ******  * **************

SG1.1          CCTCAAGCGAGTCCGAATCAGACGAAGAACAATCTGCTCCTCAGAAGTCTGAGAAATCTC   420
SG1.2          CTTCAAGCGAGTCCGAATCAGACGAAGAACAGTCTGCCCCTCAGAAGTCTGAGAAGTCTC   420
SG1.3          CTTCAAGCGAGTCCGAATCAGACGAAGAACAGTCTGCCCCTCAGAAGTCTGAGAAGTCTC   420
SG2.1          CTTCAAGCGAGTCCGAATCAGACGAAGAACAGTCCGCTCCTCAGAAGTCTGAGAAGTCTC   420
SG2.2          CTTCAAGCGAGTCCGAATCAGACGAAGAACAGTCCGCTCCTCAGAAGTCTGAGAAGTCTC   420
SG2.3          CTTCAAGCGAGTCCGAATCAGACGAAGAACAATCTGCTCCCCAGAAGTCTGAGAAGTCTC   420
OK662577.1     CTTCAAGCGAGTCCGAATCAGACGAAGAACAATCTGCCCCTCAGAAGTCTGAGAAGTCTC   420
KX883984.1     CTTCAAGCGAGTCCGAATCAGACGAAGAACAATCTGCCCCTCAGAAGTCTGAGAAGTCTC   420
               * ****************************** ** ** ** ************** ****

SG1.1          AGACGCGAGTTGCTAGGAAATCTAAGCAATCCGCACCAGAGAAGAAGGAGCGTCCTAACA   480
SG1.2          AGACGCGGGTCGCTAGGAAATCCAAGCAGTCCGCACCCGAGAAGAAGGAGCGATCTAACA   480
SG1.3          AGACGCGGGTCGCTAGGAAATCCAAGCAGTCCGCACCCGAGAAGAAGGAGCGATCTAACA   480
SG2.1          AGACGCGAGTTGCTAGGAAATCTAAGCAATCCGCACCCGAGAAGAAGGAGCGTCCTAACA   480
SG2.2          AGACGCGAGTTGCTAGGAAATCTAAGCAATCCGCACCCGAGAAGAAGGAGCGATCTAACA   480
SG2.3          AGACGCGTGTTGCTAGGAAATCTAAGCAATCTGCACCCGAGAAGAAGGAGCTTCCTAACA   480
OK662577.1     AGACGCGAGTTGCTAGGAAATCCAAGCAATCCGCACCCGAGAAGAAGGAGCGATCTAACA   480
KX883984.1     AGACGCGAGTTGCTAGGAAATCTAAGCAATCCGCACCCGAGAAGAAGGAGCGATCTAACA   480
               ******* ** *********** ***** ** ***** **************   ******

SG1.1          CC    482
SG1.2          CC    482
SG1.3          CC    482
SG2.1          CC    482
SG2.2          CC    482
SG2.3          CC    482
OK662577.1     CC    482
KX883984.1     CC    482
               **
```

Supplementary Fig. S1. Clustal Omega alignment of the sequences of 482 bp-amplicon obtained using the method herein from specimens of Indo-Pacific (SG1) and America (SG2) origin with the two

GenBank records for WZV8 (KX883984.1) and *Pv*PV (OK662577.1) from China. The gaps in the line of asterisks indicate regions of difference among the 8 sequences, while the grey background nucleotides highlight minority nucleotide differences among the eight sequences. The % identities are shown in Table 2.

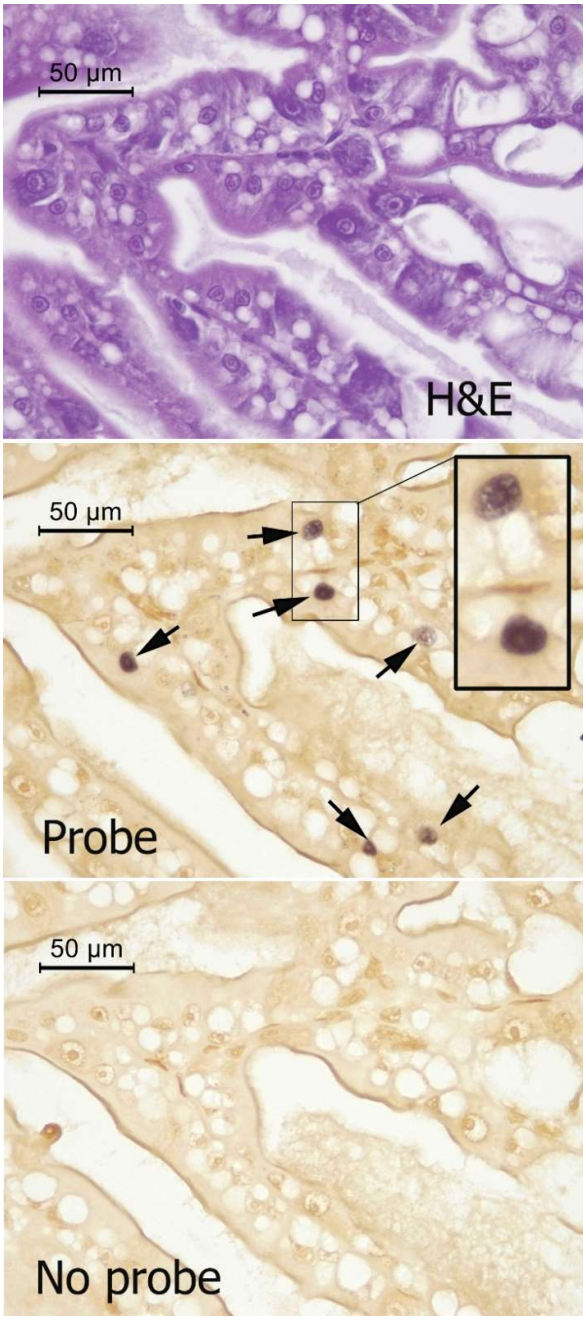

Supplementary Fig. S2. Photomicrographs of positive *in situ* hybridization signals for WZV8 (arrows) in morphologically normal nuclei of tissue in the medial area of the hepatopancreas of a shrimp specimen positive for WZV8 by PCR. The insert shows 2 of the nuclei magnified to reveal more details.

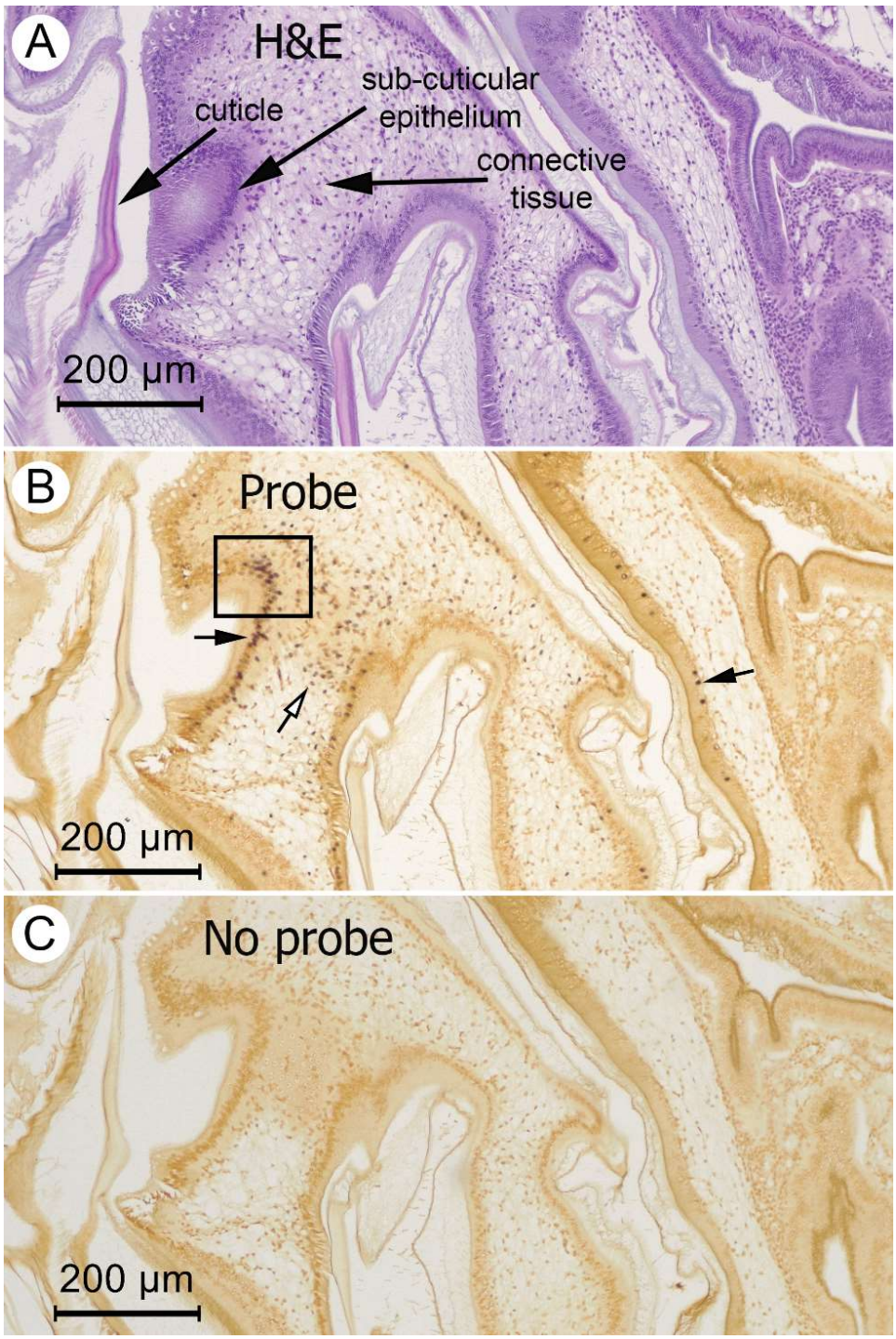

Supplementary Fig. S3. Photomicrographs of positive *in situ* hybridization signals for WZV8 (arrows) in morphologically normal nuclei of the stomach subcuticular epithelium (black arrows) and connective tissue (white-filled arrow) form a WZV8 specimen positive for WZV8 by PCR. The box in B is enlarged for more detail in insert shows 2 of the nuclei magnified to reveal more details.

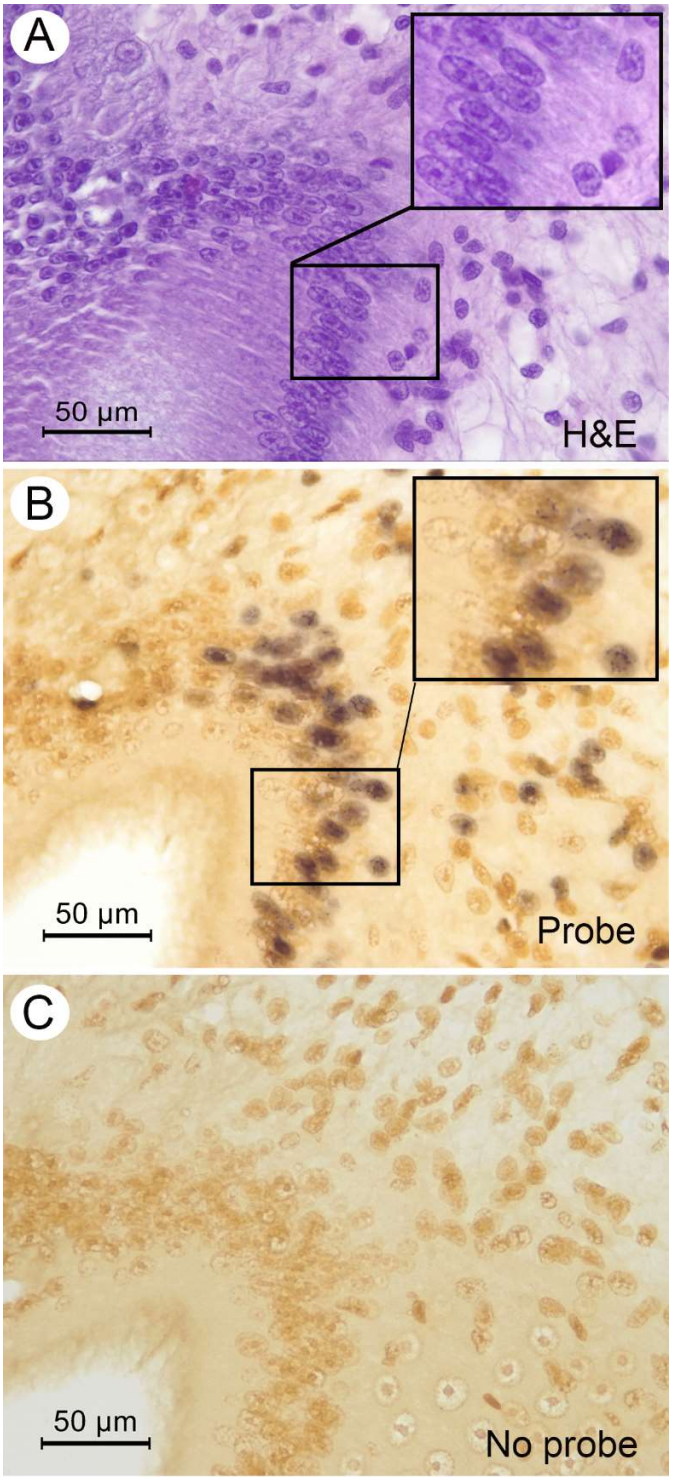

Supplementary Fig. S4. Enlarged box from Fig. S3B to show more histological details.